ADVANCED FUNCTIONAL MATERIALS
www.afm-journal.de

Preparation of Highly Ordered Nitrogen-Containing Mesoporous Carbon from a Gelatin Biomolecule and its Excellent Sensing of Acetic Acid

*Gurudas P. Mane, Siddulu N. Talapaneni, Chokkalingam Anand, Shaji Varghese, Hideo Iwai, Qingmin Ji, Katsuhiko Ariga, Toshiyuki Mori, and Ajayan Vinu**

Novel nitrogen-containing mesoporous carbon with well-ordered pores (NMC-G) and high basicity is synthesized using a low-cost single-molecule precursor, gelatin biomolecule, and SBA-15 as a template via nanocasting method. The obtained materials are thoroughly characterized. It is found that the prepared materials have excellent textural properties such as high specific surface areas, huge pore volumes, and large pore diameters. The pore diameter of the materials can also be controlled with a simple adjustment of the pore diameter of the hard templates. The C/N ratio of the samples is calculated to be ≈6.01, which is slightly higher than that observed for mesoporous carbon nitride samples. X-ray photoelectron spectroscopy (XPS) reveals the presence of sp^2 hybridized carbon in aromatic ring structure attached to amino groups. The materials could adsorb a huge quantity of CO_2. The sensing capability of the materials with different pore diameters for different adsorbates including ethanol, acetic acid, aniline, toluene, and ammonia is also investigated. Among the materials with different pore diameters studied, the material with the highest basicity and the largest pore diameter (NMC-G-150) showed excellent sensing performance with a high selectivity of adsorption for acetic acid molecule.

1. Introduction

Since the first report on the preparation of highly ordered mesoporous carbon (CMK-1) via nanocasting approach,[1] literature spread out in many orders to invent useful porous media as a potential aspirant for the future technology. Mesoporous carbon materials, due to their excellent textural characteristics and stability, have been productively utilized in catalysis, adsorption and separation of toxic molecules, fuel and solar cells, and biomedical and energy storage devices.[1–10] In addition, the excellent chemical, mechanical, and hydrothermal stability of these materials attract them as potential candidates for industrial applications including catalysis and adsorption. However, in most of the cases, the materials seem to be highly hydrophobic and only a limited number of specific active sites are available for selective sensing and catalytic applications. It is expected that the introduction of heteroatoms such as B, N and O in the carbon framework can boost not only the material performance in catalysis or sensing but may also completely change the electronic properties of the materials that are critical for various applications including semiconducting, field emission, optical, electronic devices and fuel cells.[11–22]

Although there has been a significant interest in the preparation of nitrogen doped nonporous materials owing to their excellent electronic and electrical properties, the reports on the

G. P. Mane, S. N. Talapaneni, Dr. C. Anand, S. Varghese, H. Iwai, Dr. Q. Ji, Prof. K. Ariga, Prof. A. Vinu
International Center for Materials Nanoarchitectonics
World Premier International (WPI) Research Center for Materials Nanoarchitectonics (MANA)
National Institute for Materials Science
1-1 Namiki, Tsukuba 305-0044, Ibaraki, Japan
E-mail: a.vinu@uq.edu.au

G. P. Mane, S. N. Talapaneni, Prof. T. Mori
Graduate School of Science
Department of Chemistry
Hokkaido University
Sapporo 060-0810, Japan

Dr. C. Anand, S. Varghese, Prof. A. Vinu
Australian Institute for Bioengineering and Nanotechnology
The University of Queensland
Brisbane 4072, QLD, Australia
E-mail: a.vinu@uq.edu.au

Dr. T. Mori
Hetero-interface design group
Global Research Center for Environment and Energy based on Nanomaterials Science (GREEN)
National Institute for Materials Science
1-1 Namiki, Tsukuba 305-0044, Ibaraki, Japan

DOI: 10.1002/adfm.201200207

preparation of nitrogen doped mesoporous carbon materials are quite limited. Generally, the nitrogen doped mesoporous carbon materials are prepared employing petrochemically derived materials such as acetonitrile,[19] melamine,[20] acrylonitrile,[21] diaminobenzene,[18] aniline[17] etc. as the precursors for carbon and nitrogen. For example, Kyotani et al. reported the preparation of nitrogen containing porous carbon with well ordered structure using zeolite Y as a template along with furfuryl alcohol and acetonitrile as the source for carbon and nitrogen, respectively.[15] On the other hand, Vinu et al. used a simple polymerization technique to prepare mesoporous carbon nitride by mixing ethylenediamine and carbon tetrachloride inside the nanochannels of the mesoporous silica templates such as SBA-15 and SBA-16.[16] They also demonstrated that the textural parameters of the prepared mesoporous carbon nitrides can be controlled with a simple adjustment of the degree of polymerization by tuning the ratio of the carbon and nitrogen precursors.[23] Recently Vinu et al. have also demonstrated the synthesis of partially graphitic 3D nitrogen-doped mesoporous carbon through a nanocasting approach using KIT-6 as a template and aniline as the source for both carbon and nitrogen.[17]

Diaminobenzene (DAB) has also been used as the precursor for both carbon and nitrogen for making nitrogen doped mesoporous carbon by Liu et al. who further demonstrated that the reaction temperature and the amount of the precursor play a critical role in controlling the texture and the nitrogen content of the materials.[18] Unfortunately, in most of the cases, the researchers have adopted two step strategy which involves the infiltration of the precursor first and then the subsequent polymerization of the molecule inside the pores or on the external surface. This strategy often develops the defects in the polymer network inside the porous matrix and creates textural mesopores or disordered porous CN framework. In addition, the formation of continuous polymer network may not be possible with this strategy which may even affect the nitrogen content of the final product. These drawbacks can be overcome by the direct use of the precursors with a high molecular weight and nitrogen content. However, unfortunately, there has been no report available on preparation of highly ordered nitrogen doped mesoporous carbon materials by using a CN precursor with a high molecular weight and nitrogen content as the precursor for both the carbon and nitrogen via nanocasting approach using mesoporous silica as a template.

Gelatin is a mixture of the water-soluble proteins and peptides with a high average molecular weight (ca. 50 000–80 000), produced from the partial hydrolysis of collagen that are generally extracted from the boiled bones and connective tissues of some animals. It is highly economical as it is a naturally abundant and sustainable resource with a high solubility in polar solvents. In addition, it has a large number of free NH_2 groups which may be used as the basic sites for various basic catalyzed transformations. As gelatin is very cheap material with a high molecular weight and nitrogen content, we decided to make the nitrogen doped mesoporous carbon using such a low cost CN precursor.

Here we report for the first time a simple and novel route for the preparation of nitrogen containing mesoporous carbon (NMC-G) with different pore diameters using naturally derived gelatin as a single molecule precursor for both carbon and nitrogen via nanocasting approach wherein 2D hexagonal SBA-15 with different pore diameters prepared at different hydrothermal temperature were used as the hard templates. We demonstrate that the gelatin biomolecule could be easily converted into well-ordered NMC-G materials with a high surface area and a nitrogen content. The nitrogen atoms are located in the wall structure of the mesoporous carbon in the form of NH or NH_2 groups that are orginated from the aminogroups present in the gelatin biomolecule. We also demonstrate that the NMC exhibits a high basicity and can adsorb huge quantity of CO_2 molecules which is slightly acidic. The sensing properties of the NMC sample employing quartz crystal microbalance (QCM) technique for different molecules including acetic acid, aniline, ammonia, ethanol and toluene have been investigated. The NMC-G samples showed a high selectivity for the sensing of the acetic acid molecules due to the strong acid-base interaction between the free NH or NH_2 groups available on the surface of the walls structure of the sample and the COOH groups from the acetic acid.

2. Results and Discussion

The pore structural order of the NMC-G materials was analyzed by using powder XRD measurements. Although the molecular size of the precursor is quite large, the pore diameter of the hard template, SBA-15 (ca. 9 nm) can accommodate such a large molecule easily without any mass diffusion problem. The perfect filling of the pores with the precursor molecule is extremely important in order to get the well ordered porous structure. In this case, SBA-15 template can solve this problem as it is perfect template that can offer the large pore diameter. **Figure 1** shows powder XRD patterns of NMC-G samples prepared from gelatin biomolecule. All the materials exhibit three clear peaks that can be indexed to the (100) and (110) reflections of the highly ordered two dimensional hexagonal mesostructure with the space group of *p6mm* that almost similar to that of the XRD pattern of the parent SBA-15 silica template which consists

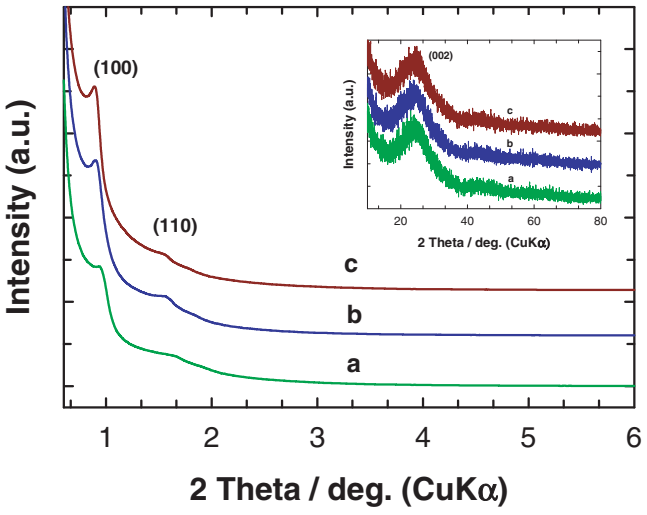

Figure 1. Powder XRD patterns of nitrogen containing mesoporous carbon with various pore diameters prepared form SBA-15-x templates: a) NMC-G-100, b) NMC-G-130, and c) NMC-G-150). Insets: Higher angle XRD patterns of: a) NMC-G-100, b) NMC-G-130, and c) NMC-G-150.

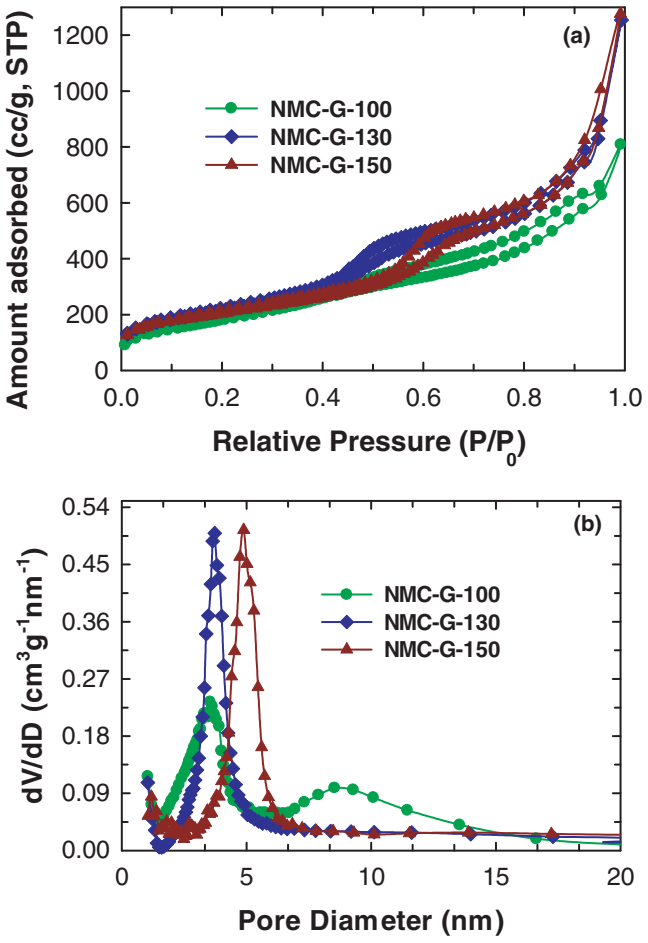

Figure 2. a) Nitrogen adsorption-desorption isotherms and b) BJH pore size distribution of NMC-G-100, NMC-G-130, and NMC-G-150 samples.

of a hexagonal arrangement of cylindrical pores. Remarkably, the position of the main peak varies significantly with the pore diameter of the SBA-15 template used. It has been observed that an increase in the pore diameter of the template causes a shift of the peak towards lower angle region which provides evidence of increase of d-spacing and the unit cell parameter. Similar results were also obtained for the MCN-1 samples with different pore diameters which were prepared by using SBA-15 as different templates via a simple chemical polymerization of ethylenediamine and carbon tetrachloride.[16,23] Interestingly, all the samples show a single broad diffraction peak near 25.6° which corresponds to an interlayer d-spacing of 0.362 nm. This peak is almost similar to the characteristic (002) basal plane diffraction peak in the non-porous carbon nitride materials, revealing that the presence of turbostratic ordering of carbon and nitrogen atoms in the graphitic layers of NMC-G samples. It should be noted that the interlayer distance is slightly higher than that of pure graphitic carbon which could be due to either the defect sites or curvature of the carbon walls or the partial crystallization of carbon framework.

Textural parameters and mesoscale ordering of the materials were obtained by nitrogen adsorption-desorption measurements. **Figure 2**a shows the N_2 adsorption-desorption isotherms

Table 1. Textural parameters of nitrogen containing mesoporous carbons with different pore diameters.

Sample name	d_{100} [nm]	a_0 [nm]	A_{BET} [m^2/g]	Pore volume[a)] [$cm^3\ g^{-1}$]	Pore diameter[b)] [nm]
NMC-G-100	9.29	10.72	764	1.14	3.54
NMC-G-130	9.72	11.22	781	1.28	3.72
NMC-G-150	9.92	11.45	804	1.40	4.89

[a)]Total pore volumes estimated from the adsorbed amount at a relative pressure of $P/P_o = 0.99$; [b)]Pore diameters derived from the desorption branches of the isotherms by using the BJH method.

of the NMC-G-X materials prepared using SBA-15 templates with different pore diameters. All of the isotherms are of type IV according to IUPAC classification and exhibit H1 hysteresis with a featured capillary condensation in the mesopores, indicating the presence of well ordered mesopores in all the samples. Figure 2b shows the BJH desorption pore size distribution of NMC-G-100, NMC-G-130, and NMC-G-150. As can be seen in Figure 2b, all the samples show a narrow pore size distribution and the pore size increases with increasing the pore diameter of the silica template used. The pore diameter increases from 3.54 to 4.89 nm with increasing the synthesis temperature of the template from 100 to 150 °C, respectively. These results reveal that the pore size tuning is possible even with the use of the gelatin biomolecule as a CN precursor. The specific surface area, the specific pore volume, and the pore diameter of the samples prepared using SBA-15 with different pore diameters as templates are given in **Table 1**. The materials exhibit high surface areas (712 to 804 m^2/g) and large pore volumes (1.14 to 1.40 cm^3/g) and these large values of the physical parameters together with a sharp capillary condensation step clearly reflect the presence of the well-ordered mesoporosity in the sample. It should also be noted that the specific surface area and the specific pore volume of the samples increase with increasing the pore diameter of the hard template. The specific surface area is 712 m^2/g for NMC-G-100, which increases to 804 m^2/g for NMC-G-150 whereas the specific pore volume increases from 1.14 to 1.40 cm^3/g for the same samples. Among the materials studied, NMC-G-150 registered the highest pore volume, specific surface area and the largest pore diameter.

The successful replication of 2D hexagonal SBA-15 template in the NMC-G materials prepared from the gelatin biomolecule can be observed with the help of high resolution scanning electron microscopy (HR-SEM) and high resolution transmission electron microscopy (HR-TEM) techniques. **Figure 3** shows the representative HR-SEM images of NMC-G-150. A highly ordered mesopores which are arranged in an orderly fashion with a regular interval was observed for the NMC-G-150, confirming that the replication process was successful and the mesostructure and the ordered nature of the pores are completely replicated into the nitrogen doped mesoporous carbon. As can also be seen in Figure 3, the low resolution SEM image of NCM-G-150 displays rod like morphology, which are stacked together in an orderly fashion, similar to that of the ordered mesoporous silica. However, the particles are joined together with the proper interval which made the particle much bigger

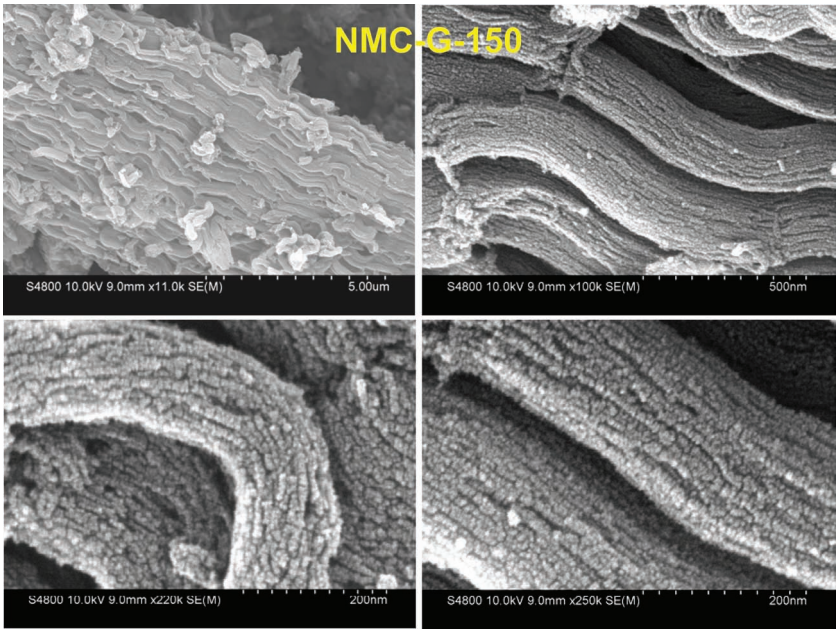

Figure 3. HR-SEM images of NMC-G-150.

than that of the SBA-15. This indicates that the gelatin precursor polymerizes with the neighbouring particles through a simple dehydration process. However, the pore structure was still retained even after the removal of the mesoporous silica template. The particles are highly uniform and the width of the particles is in the range of 80 to 100 nm whereas length of the particles varies from 500 nm to a few micrometers. The pore size of the materials was also calculated using the HR-SEM images which is almost similar to that obtained from the nitrogen adsorption isotherm.

The representative HRTEM images of the NMC-G-150 are also shown in **Figure 4**. Bright contrast strips on the under focused image represent the pore wall images, whereas dark contrast cores display empty channels. The porous structure of the sample when viewed in the direction perpendicular to their axis, displays a linear array of mesopores arranged in a regular pattern. However, when viewed down the pore axis, the sample reveals a hexagonally ordered honey-comb like structure with a uniform mesoporous channels, similar to that of the highly ordered SBA-15. These well ordered mesopores are originated from the silica walls that are dissolved with a 5 wt% of HF in water. The pore diameter calculated from the HR-TEM images which show a linear arrays of mesopores with a regular interval is almost similar to that obtained from the nitrogen adsorption measurement. It should be noted that a well-ordered mesoporous matrix is seen throughout the sample, revealing the purity and the uniformity of the ordered porous matrix in the nitrogen doped mesoporous carbon sample. In order to check the nature and the co-ordination and the amount of the nitrogen content in the wall structure of the NMC-G materials, the samples were analyzed with electron energy loss (EEL) spectroscopy. **Figure 5** shows the representative EEL spectrum of NMC-G-150 sample which clearly shows the presence of carbon and nitrogen atoms in the sample. However, there is a minor and broad peak corresponding to oxygen was observed at higher eV although a significant amount of oxygen present in the CN precursor used for the synthesis of NMC-G. These results reveal that the oxygen content in the sample is low. The sample displays C-K and N-K ionization edges which are located at 284 and 401 eV respectively. The peak at 284 eV is due to π^*edge, corresponding to a 1s–π^* transition, closely resembling the features of the material with the sp^2 hybridised carbon like graphene or graphite. This transition is due to the higher electronegativity of nitrogen atoms that decreases the electron density on the carbon atoms. From the shape and the intensity of the C and N-K edges, one can clearly see a strong bonding interaction between the C and N species in the sample. The N-K edge peak in the EEL spectrum also indicates that the nitrogen atoms are mostly sp2 hybridized with carbon. Similar type of spectrum has also been reported for mesoporous carbon nitride samples such as MCN-1, MCN-2, and MCN-3.[16a,b,24]

Chemical composition, nature of bonding, and purity of the sample were examined by XPS analysis. XPS spectrum of

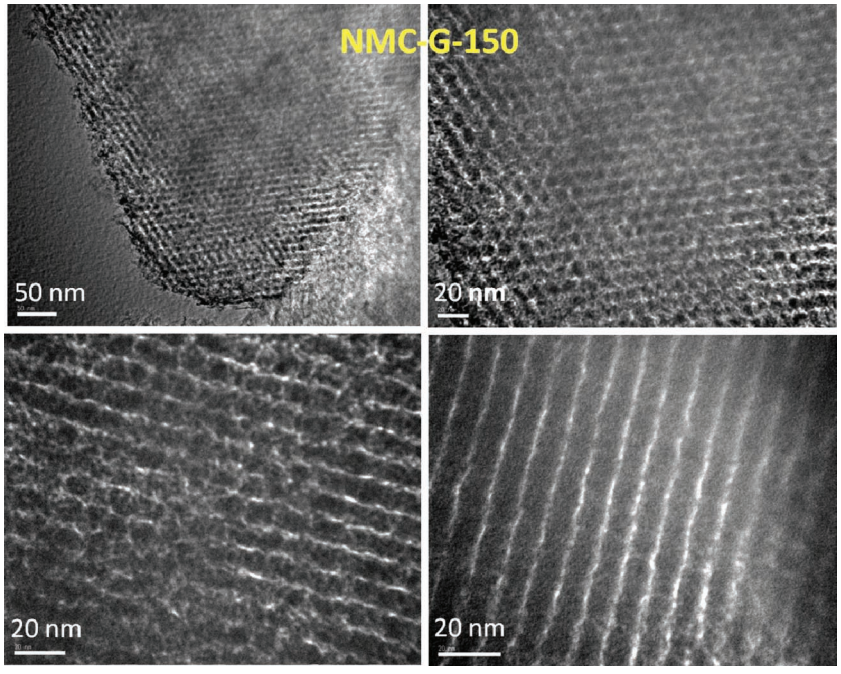

Figure 4. HR-TEM images of NMC-G-150.

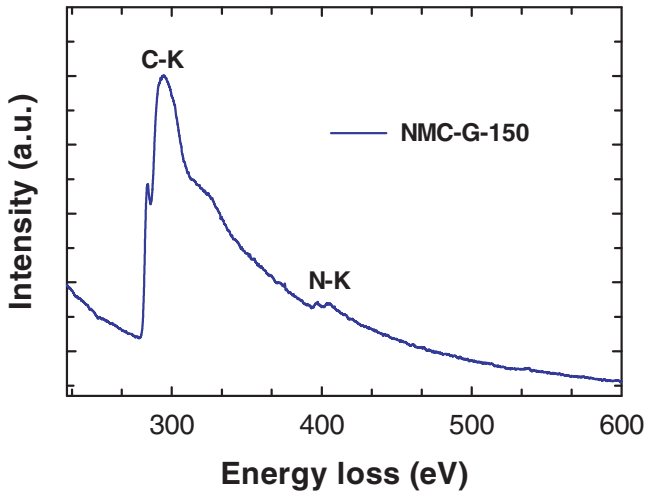

Figure 5. EEL spectrum of a NMC-G-150 sample.

NMC-G-150 (Figure S1, Supporting Information) shows the presence of carbon, nitrogen and oxygen. The existence of oxygen can be attributed to the presence of moisture, atmospheric O_2, oxygen from the CN precursor, or CO_2 adsorbed on the surface of NMC-G-150. It should be noted that the sample contains a small amount of the F atom which comes from the HF acid used for the removal of the silica template. However, after the repeated washing, the F ions can be completely removed. **Figure 6**a,b shows the high resolution C 1s and N 1s spectra of NMC-G-150. The C1s spectrum can be deconvoluted into the three well resolved peaks with binding energies of 284.3 eV, 285.7 eV and 289.1 eV which were very close to the values reported for non-porous carbon nitride samples.[25] The peaks at 284.3 eV and 285.7 eV correspond to the pure graphitic sites in the CN matrix and sp^2 carbon atoms bonded to nitrogen inside the aromatic ring, respectively[26,27] whereas the peak at 289.2 eV is assigned to the sp^2 hybridized carbon in the aromatic ring attached to the primary ($-NH_2$) or secondary (-NH-) groups.[26] N1s spectrum (Figure 6b) shows three peaks centred at 398.2, 400.1, and 404.5 eV which could be attributed to the pyrole-like nitrogen atoms incorporated into graphitic sheets or sp^2 nitrogen bonded to carbon,[21,22,24] N atoms trigonaly bonded to all sp^2 carbons,[25] and pyridinic N^+- O^-, or N-N bonds,[21,27] respectively. These results reveal that the wall structure of the sample contains a lot of nitrogen atoms which are linked with both the five and six membered aromatic ring and further attached within the ring or outside the ring. The C/N ratio of the sample estimated from XPS analysis is (ca. 6.57 ± 0.05) which reveals that the nitrogen content of the sample is slightly lower than that of the MCN family.[16a,b,24] It should be noted that the nitrogen content of the sample was also compared with the data obtained from the CHNO and EELS analysis. The C/N ratio obtained from the XPS measurement is almost consistent that obtained from other measurements such as CHNS which registered the C/N ratio of ca. 6.8 ± 0.2.

The purity and the amount of nitrogen present in the samples were also investigated by energy dispersive X-ray spectroscopy (EDS) measurement (**Figure 7** and Figure S2, Supporting Information). Figure 7 shows EDS pattern for NMC-G-150.

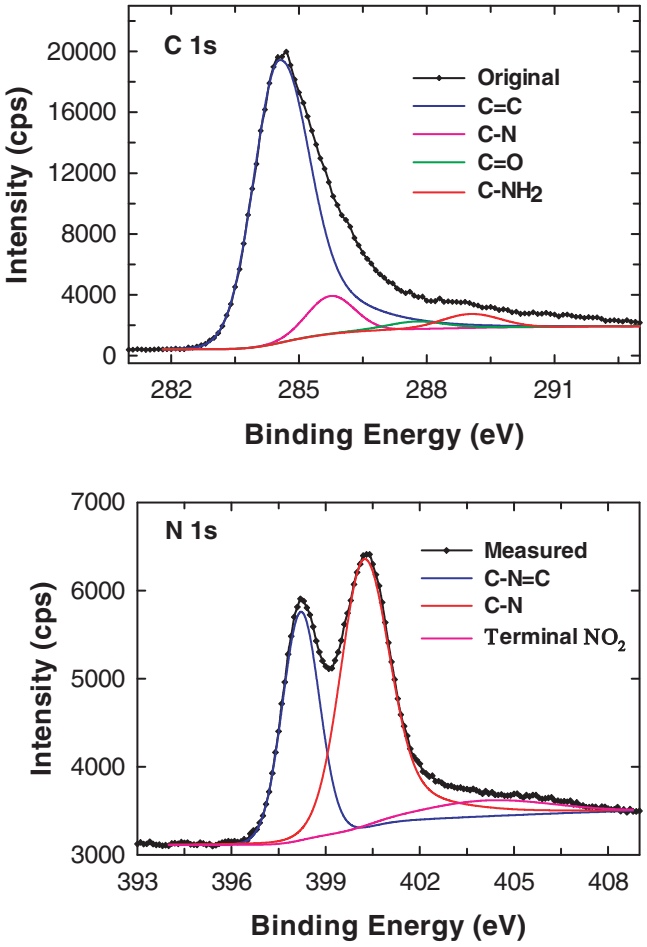

Figure 6. a) C1s and b) N1s XPS of NMC-G-150 sample.

Peaks for the elements C, N, O are clearly seen in the EDX spectrum, indicating that the sample is indeed doped with a high content of nitrogen. The amount of nitrogen is calculated to be 14.46 at% (C/N ratio–6.01), which is somewhat lower than

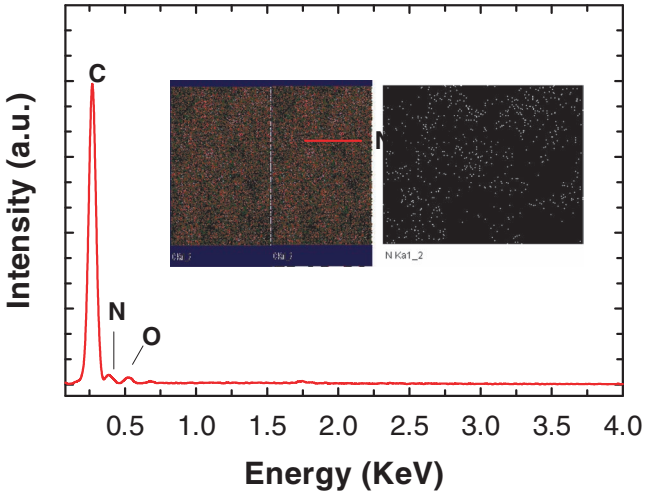

Figure 7. EDX analysis and the elemental mapping of NMC-G-150 sample.

that obtained from the XPS and CHN analysis. Although the CN precursor offers a huge amount of nitrogen for the fabrication of NMC-G, we could not achieve the preparation of materials with C_3N_4 symmetry. The low amount of nitrogen in the final product is due to a low thermodynamic stability of the nitrogen in the carbon matrix at high temperature and the nitrogen prefers to stays as a molecule. As a result, the nitrogen is coming out of the CN framework at high temperature, resulting in a low nitrogen content. In addition, the majority of nitrogen atoms in gelatin biomolecule are present in the linear chain structure (Supporting Information, Scheme S1) which supports the decomposition of loosely bound nitrogen atoms from linear chains at a high carbonization temperature, leaving behind the final product with a low nitrogen content. Although the nitrogen content of the materials is lower than that of the theoretically predicted nonporous carbon nitride, it is almost close to that observed for the previously reported carbon nitride materials with a porous structure including MCN-1, MCN-2, and MCN-3.[16,23,24]

As we found that NMC-G materials have a reasonable amount of nitrogen in the carbon matrix, we tried to investigate the basic characteristics of the materials through a simple temperature programmed desorption (TPD) using CO_2 as a probe molecule. This method is often used for the calculation of the number of basic sites on the surface of the nitrogen doped carbon materials. In addition, the strength of the basic sites can be calculated from the desorption temperature at which the CO_2 molecules are desorbed and the area under the peak at different temperature.[29] As the temperature of the system exceeds the binding energy (enthalpy of adsorption) of the adsorbed species, it starts to desorb from the surface as the bonding between the CO_2 molecule and the surface is broken and guided by the carrier gas to the detector.[28] The TPD of CO_2 spectrum for the NMC-G-150 in comparison to NMC-G-100 is shown in **Figure 8**. The sample displays a broad peak centered at 173 °C at which the desorption of the CO_2 molecules is very high. Prior to the desorption measurement, the sample was allowed to adsorb

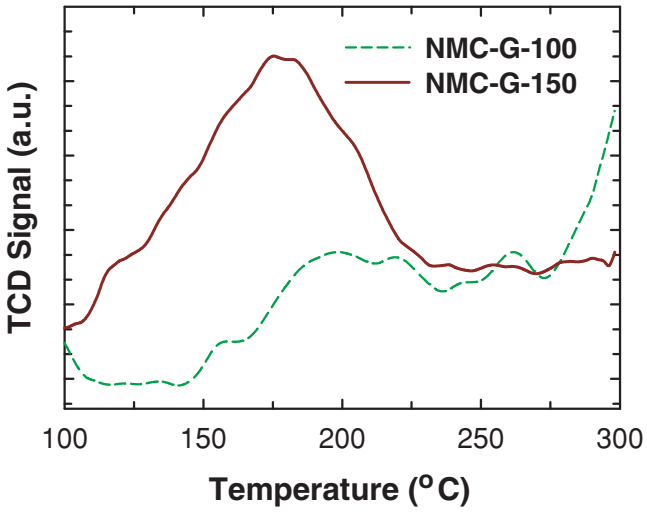

Figure 8. Temperature programmed desorption (TPD) plot of CO_2 of NMC-G-100 (dashed line) and NMC-G-150 (solid line).

CO_2 molecule at the adsorption temperature of 100 °C. After the adsorption process, the sample was flushed with a He gas in order to remove the loosely bounded CO_2 molecules from the surface of the adsorbent. From the shape of the peak, one can clearly say that the sample adsorbed a huge quantity of the CO_2 molecules which clearly reflects the basic nature of the sample. Since the area under the peak is proportional to the density of CO_2 molecules adsorbed on the surface of the sample, we calculated the amount of the CO_2 liberated from the pore channels of the NMC-G and it is well clear that the sample could retain a huge amount of the adsorbed CO_2 molecules even at a high temperature and the amount of the CO_2 desorbed from the NMC-G is calculated be 0.185 mmol of CO_2 per gram of the NMC-G-150. The reason for such a significant adsorption of CO_2 molecules can be attributed to the existence of lot of basic sites (-NH_2, -NH- groups) on the surface of the sample which encourages the interaction with the slightly acidic CO_2 molecules through a simple acid-base interaction. These data reveal that the NMC-G-150 sample is highly basic in nature due to the presence of nitrogen atoms attached to the carbon matrix and is a good adsorbent for the capture of the CO_2 molecules even at a high temperature. The TPD of CO_2 profiles of NMC-G sample with different pore diameters are also compared (Figure 8). Among the samples studied, NMC-G-150 registered the highest amount of CO_2 adsorption, revealing that the basicity of the NMC-G-150 (0.185 mmol of CO_2/g) is much higher than that of other samples. The basicity of the samples is in the range of 0.12 for NMC-G-100 to 0.185 mmol of CO_2/g for NMC-G-150. These findings not only reveal that the material is highly basic but also a good adsorbent for the capture of CO_2 molecules.

As these materials exhibit high surface area together with a lot of free NH_2 groups on the surface of the pore walls, we tried to use them as the supports for the sensing of different adsorbates such as ethanol, acetic acid, aniline, toluene, and ammonia. Quartz crystal microbalance (QCM) has been used for the sensing applications. QCM is an ultrasensitive thickness shear mode (TSM) device that consists of single crystal quartz plate with thin film metal electrodes on each surface.[31] This piezoelectric quartz crystal can be made to oscillate at its resonance frequency when attached to externally driven oscillator circuit. Principle of operation depends on the Saurbrey equation which states that, the mass added to or removed from the surface (Δm) of the electrode induces the frequency shift (Δf). The use of QCM as chemical sensors has been well documented for various toxic and hazardous vapors.[30,31] However, there has been no report available in the literature on the QCM sensing studies using the nitrogen doped porous carbon materials. Initially the samples were mounted on a QCM plate before the sensing measurements. **Figure 9**a displays the typical response patterns obtained from the QCM sensor showing very fast response and well reversibility when the NMC-G-150 sample is exposed to the vapors of different adsorbates such as ethanol, acetic acid, aniline, toluene, and ammonia whereas the Figure 9b shows the magnitudes of frequency shift for different vapors. Different amplitudes of frequency shift can be seen for different adsorbates such as ethanol, acetic acid, aniline, toluene, and ammonia and other organic acids such as formic acid, acrylic acid, propionic acid and octanoic acid. Among the adsorbates studied, NMC-G-150 showed a huge frequency shift for the toxic acetic acid

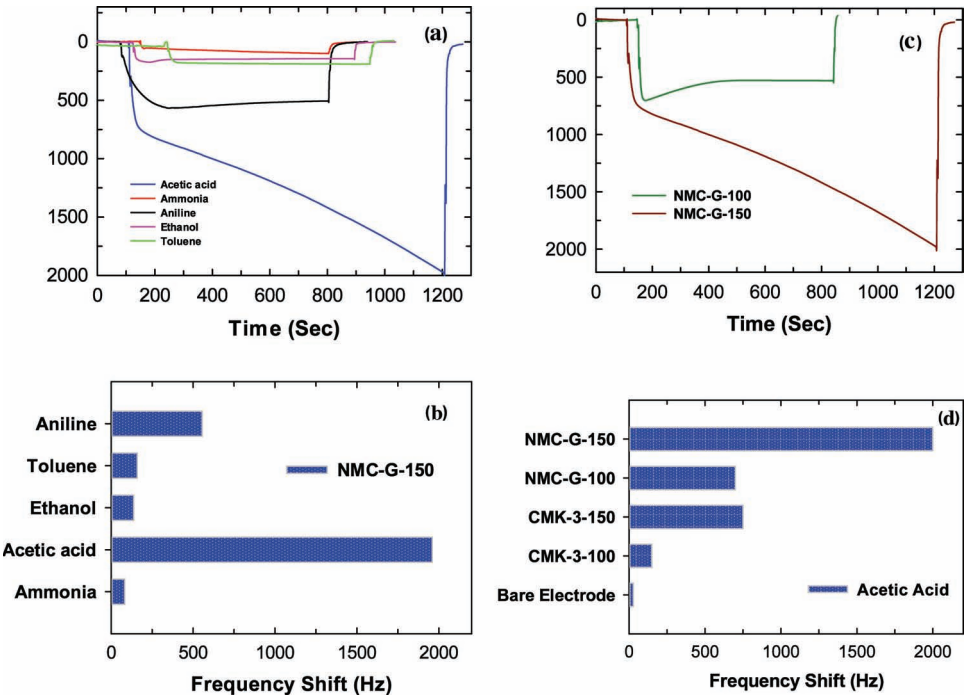

Figure 9. a) The response of NMC-G-150 coated QCM sensor to the exposure of different organic vapours, b) bar graph representing the magnitude of frequency shift of different organic vapors for NMC-G-150, c) comparison of the sensing performance of the NMC-G-150 and NMC-G-100, and d) bar graph representing the magnitude of frequency shift for acetic acid sensing with different supports.

molecule, revealing a high selectivity of sensing for the acetic acid molecules (Figure 9 and Figure S4, Supporting Information). Among the organic acid gases studied, acetic acid seems to have a superior affinity towards the NMC-G-150. As can be seen, the selectivity of the sensing of different organic acid gases over NMC-G-150 decreases in the following order: acetic acid > formic acid > acrylic acid > propionic acid > octanoic acid.

The QCM curve shows a rapid frequency drop for the acetic acid which can be attributed to the adsorption of the adsorbate on the outer surface of the film and the subsequent frequency drop is due to the penetration (diffusion) of the vapor molecules inside the porous channels of the sample and adsorbed on the active adsorption sites available in the pore wall structure. As can be seen in Figure 9, the adsorption of acetic acid over the NMC-G-150 is very high and such a massive uptake of toxic acetic acid molecule has never been reported in the open literature so far and the extraordinary performance can be explained with two reasons. One of the main reasons behind the massive uptake of the acetic acid molecules is due to the strong acid base interaction between the acid groups of the adsorbate and the free and highly basic sites such as NH or NH_2 groups on the surface of the pore wall structure of the NMC-G-150. Another reason is that the adsorbent possesses a high surface area, a large pore volume, and the largest pore diameter which offer a huge number of adsorption sites together with the free NH_2 groups that significantly enhance the host-guest interaction and provide enough room for the storage. With the best of our knowledge, this is the first report on the highly selective sensing performance of the nitrogen doped mesoporous carbon materials that create a platform for developing sensing device for the adsorption of various toxic molecules. In order to understand the role of the pore diameter, pore volume and the specific surface area, we performed the QCM sensing measurements over NMC-G-100, NMC-G-150, CMK-3-150, CMK-3-100, and a bare QCM electrode. Among the samples studied, NMC-G-150 showed the highest performance with a highly selective sensing towards the acetic acid. It should also be noted that the nitrogen doped mesoporous samples displayed much higher selectivity of acetic acid adsorption than those of the mesoporous carbon samples. This clearly reveals role of the nitrogen atom in the pore wall structure of the NMC-G samples which helps the adsorption of the acetic acid molecules along the nitrogen doped carbon pore walls.

3. Conclusions

In summary, we have synthesized well-ordered nitrogen containing mesoporous carbon with tunable pore diameters by using a low cost and naturally abundant gelatin biomolecule as a CN precursor via nanocasting technique with mesoporous silica SBA-15 with different pore diameters as hard templates. The obtained materials exhibit high nitrogen content together with a well-ordered structure, a high surface area, a large pore volume, and tunable pore diameters. EDS, EELS, CHNO, and XPS analysis revealed that the materials indeed contain a quite a lot of nitrogen content which offers a huge number of basic sites on the surface of the pore walls. We also demonstrated the basic characterisitic of the materials with the help of TPD of CO_2 and the basicity of the materials is calculated to be in the range of 0.12 to 0.185 mmol of CO_2 per gram of the adsorbent. We also demonstrated the sensing properties of the NMC-G-150

employing QCM technique for various adsorbates such as ethanol, acetic acid, aniline, toluene, and ammonia. The material showed a high selectivity of sensing for the acetic acid with a huge frequency shift (2000 Hz) due to a strong acid-base interaction between the acid groups of the adsorbate and the free NH_2 groups on the adsorbent. These findings reveal that novel mesoporous carbon materials with high nitrogen and excellent textural parameters can be synthesized with a low cost CN precursor which makes the whole process simpler and a low cost and this strategy can be applied for the fabrication of series of NMC-G materials with different structure and morphology. Moreover, the NMC-Gs are proved to be the potential candidates for the sensing of the toxic molecules including CO_2 and acetic acid which may trigger the potential possibility of the materials for sensing various toxic acidic molecules and further widen the scope of the materials for various applications including basic and photocatalysis, and for the capture of the CO_2 molecule.

4. Experimental Section

Materials: All chemicals used in this study were analytical grade and used as produced without any further purification. Tetraethyl orthosilicate (TEOS) and gelatin were obtained from Aldrich and Nacalai Tesque respectively. Concentrated sulfuric acid (H_2SO_4) was obtained from Nacalai Tesque.

Preparation of SBA-15 with various pore diameters: The synthesis of SBA-15 with various pore diameters using the poly(ethylene glycol)-block-poly(propelyne glycol)-block-poly(ethylene glycol) ($EO_{20}PO_{70}EO_{20}$, a average molecular weight 5800, Aldrich) amphiphilic triblock copolymer was carried out using the procedure reported by Vinu et al.[4b] Synthesis was carried out as below: 4 g of amphiphilic trblock copolymer was dispersed in water (30 g) and HCl solution (120 ml, 2 M) and stirred for 5 h. Thereafter, tetraethyl orthosilicate (TEOS, 9 g) was added to the homogenous solution under stirring. The resulting gel was aged at 40 °C for 24 h and finally heated to 100 °C for 48 h. The first set of samples was prepared by the procedure as described above and crystallized at different temperatures between 100 and 150 °C. The samples were labelled SBA-15-x, where x denotes the synthesis temperature. After synthesis, the obtained solids were calcined in flowing air at 540 °C to remove the polymeric surfactant in order to create well-ordered mesoporosity.

Synthesis of Nitrogen Containing Mesoporous Carbon Derived from Gelatin Protein (NMC-G): In a typical synthesis of NMC-G, 1 g of calcined SBA-15-x (x = 100 °C, 130 °C, 150 °C) was thoroughly mixed with the solution obtained by dissolving 1.0 g of gelatin and 0.168 g of H_2SO_4 in 5 g of deionised (DI) water. The mixture was placed in a drying oven for 6 h at 100 °C and subsequently the oven temperature was increased to 160 °C and kept it at the same temperature for another 6 h. The composite of silica template with partially carbonized gelatin was treated again using the above condition including the treatment at 100 °C and 160 °C for 6 hours each after the addition of 0.75 g of gelatin, 0.12 g of H_2SO_4 and 5 g of DI water. The carbonization was carried out at 600 °C in argon atmosphere. The composite obtained after carbonization was treated with HF at room temperature in order to remove the mesoporous silica template. The obtained template free nitrogen doped mesoporous carbon was filtered, washed several times with ethanol, and dried at 100 °C. The colour of the final nitrogen containng mesoporous carbon is black. For 1.75 g of gelatin boimolecules, ca. 0.6 g of the product can be recovered after the HF treatment. A second set of the samples was prepared by using the same procedure with different pore diameter SBA-15-x templates in order to control the textural parameters including the pore diameter of the final product. The samples are denoted NMC-G-X where X denotes the synthesis temperature of the template.

Characterization: The powder X-ray diffraction patterns of NMC-G-x materials were collected on Rigaku diffractometer using CuKα (λ = 0.154 nm) radiation. The patterns were recorded in the 2θ range of 0.6–10° with a 2θ step size of 0.01° and a step time of 1 s. Nitrogen adsorption desorption isotherms were measured at –196 °C on a Quantachrome Autosorb 1 sorption analyzer. All samples were outgassed for 12 h at 200 °C under vacuum ($p < 1 \times 10^{-5}$ h Pa) in the degas port of the adsorption analyzer. The specific surface area was calculated using the BET model. The pore size distributions were obtained from desorption branches of the isotherms. HRTEM images were obtained using JEOL-3000F transmission electron microscope equipped with a Gatan-776 electron energy loss spectrometer (EELS). The preparation of the samples for HRTEM involved sonication in ethanol for 5 min and deposition on copper grid. The acceleration voltage for electron beam was 200 KV. X-ray photoelectron spectroscopy (XPS) measurement was carried out in a PHI 5400 instrument with a 200 W Mg KR probe beam to characterize the sample. Prior to analysis, the samples were evacuated at a high vacuum. Survey and multiregion spectra were recorded at C1s and N1s photoelectron peaks. Each spectra region of photoelectron interest was scanned several times to obtain good signal-to-noise ratios.

Supporting Information

Supporting Information is available from the Wiley Online Library or from the author.

Acknowledgements

This work was partially supported by the Ministry of Education, Culture, Sports, Science and Technology (MEXT) under the Strategic Program for Building an Asian Science and Technology Community Scheme and World Premier International Research Center (WPI) Initiative on Materials Nanoarchitectonics, MEXT, Japan. A.V. thanks Australian Research Council for the award of Future Fellowship. S.N.T. and G.P.M. thank NIMS for the graduate fellowship. This article was modified after online publication. Reference citations on pages 3600–3601 were corrected.

Received: January 22, 2012
Revised: March 16, 2012
Published online: May 18, 2012

[1] R. Ryoo, S. H. Joo, S. Jun, *J. Phys. Chem. B* **1999**, *103*, 7743.
[2] S. H. Joo, S. J. Choi, I. Oh, J. Kwak, Z. Liu, O. Terasaki, R. Ryoo, *Nature* **2001**, *412*, 169.
[3] A. Vinu, C. Streb, V. Murugesan, M. Hartmann, *J. Phys. Chem. B* **2003**, *103*, 7743.
[4] a) A. Vinu, V. Murugesan, M. Hartmann, *J. Phys. Chem. B* **2004**, *108*, 7323; b) M. Hartmann, A. Vinu, *Langmuir* **2002**, *18*, 8010.
[5] K. Lu, D. D. L. Chung, *Carbon* **1997**, *35*, 427.
[6] S. B. Yoon, J. Y. Kim, J.-S. Yu, *Chem. Commun.* **2002**, 1536.
[7] D. Banham, F. Feng, J. Burt, E. Alsrayheen, V. Birss, *Carbon* **2010**, *48*, 1056.
[8] S. B. Yoon, J. Y. Kim, J.-S. Yu, *Chem. Commun.* **2001**, 559.
[9] J. Lee, S. Yoon, S. M. Oh, S. Shin, T. Hyeon, *Adv. Mater.* **2000**, *12*, 359.
[10] S. S. Kim, T. J. Pinnavaia, *Chem. Commun.* **2001**, 2418.
[11] R. B. Sharma, D. J. Late, D. S. Joag, A. Govindaraj, C. N. R. Rao, *Chem. Phys. Lett.* **2006**, *428*, 102.
[12] a) M. Koh, T. Nakajima, *Carbon* **2000**, *38*, 1947; b) M. Kim, S. Hwang, J.-S. Yu, *J. Mater. Chem.* **2007**, *17*, 1656.
[13] F. V. Paez, A. Zamudio, A. L. Elias, H. Son, E. B. Barros, S. G. Chou, Y. A. Kim, H. Muramatsu, T. Kayashi, J. Kong, H. Terrones, G.Dresselhaus, M. Endo, M. Terrones, M. S. Dresselhaus, *Chem. Phys. Lett.* **2006**, *424*, 345.
[14] C.-M. Yang, C. Weidenthaler, B. Spliethof, M. Mayanna, F. Schüth, *Chem. Mater.* **2005**, *17*, 355.

[15] P.-X. Hou, H. Orikasa, T. Yamazaki, K. Matsuoka, A. Tomita, N. Setoyama, Y. Fukushima, T. Kyotani, *Chem. Mater.* **2005**, *17*, 5187.
[16] a) A. Vinu, K. Ariga, T. Mori, T. Nakanishi, S. Hishita, D. Golberg, Y. Bando, *Adv. Mater.* **2005**, *17*, 1648; b) A. Vinu, P. Srinivasu, D. P. Sawant, T. Mori, K. Ariga, J. Chang, S. Jhung, V. V. Balasubramanian, Y. K. Hwang, *Chem. Mater.* **2007**, *19*, 4367.
[17] A. Vinu, S. Anandan, C. Anand, P. Srinivasu, K. Ariga, T. Mori, *Microporous Mesoporous Mater.* **2008**, *109*, 398.
[18] N. Liu, L. Yin, C. Wang, L. Zhang, N. Lun, D. Xiang, Y. Qi, R. Gao, *Carbon* **2010**, *48*, 3579.
[19] A. Lu, A. Kiefer, W. Schmidt, F. Schüth, *Chem. Mater.* **2004**, *16*, 100.
[20] A. C. Pierre, G. M. Pajonk, *Chem. Rev.* **2002**, *102*, 4243.
[21] G. Liu, X. Li, P. Ganesan, B. N. Popov, *Appl. Catal. B: Environ.* **2009**, *93*, 156.
[22] [a) S. Kubo, R. J. White, N. Yoshizawa, M. Antonietti, M. Titirici, *Chem. Mater.* **2011**, *23*, 4882; b) R. J. White, M. Antonietti, M. Titirici, *J. Mater. Chem.* **2009**, *19*, 8645.
[23] A. Vinu, *Adv. Funct. Mater.* **2008**, *80*, 816.
[24] X. Jin, V. V. Balasubramanian, S. T. Selvan, D. P. Sawant, M. A. Chari, L. Qu, A. Vinu, *Angew. Chem. Int. Ed.* **2009**, *48*, 7884.
[25] [a) Y. H. Chen, B. K. Tay, S. P. Lau, X. Shi, X. L. Qiao, J. G. Chen, Y. P. Wu, Z. H. Sun, C. S. Xie, *J. Mater. Res.* **2002**, *17*, 521; b) Yu Qiu, Lian Gao, *Chem Commun.* **2003**, 2378; c) D. Marton, K. J. Boyd, A. H. Al-Bayati, S. S. Todorov, J. W. Rabalais, *Phys. Rev. Lett.* **1994**, *73*, 118.
[26] J. C. Sanchez-Lopez, C. Donnet, F. Lefebvre, C. Fernandez-Ramos, A. Fernandez, *J. Appl. Phys.* **2001**, *90*, 675.
[27] D. Marton, K. J. Boyd, A. H. Al-Bayati, S. S. Todorov, J. W. Rabalais, *Phys. Rev. Lett.* **1994**, *73*, 118.
[28] H. Hattori, *Chem Rev.* **1995**, *95*, 537.
[29] F. Reif, *Fundamentals of Statistical and Thermal Physics*, McGraw Hill, Boston, MA **1965**, pp. 331–397.
[30] J. W. Grate, *Chem Rev.* **2000**, *100*, 2627.
[31] J. W. Grate, S. J. Martin, R. M. White, *Anal. Chem.* **1993**, *65*, 940A.